Codebook-Based Precoding for SDMA-OFDMA with Spectrum Sharing

Han-Shin Jo

This paper focuses on codebook-based precoding for space-division multiple access/orthogonal frequency-division multiple access (SDMA-OFDMA) systems aiming to guarantee high throughput for their users as well as to mitigate interference to fixed satellite service (FSS). A systematic design of SDMA codebook for subband-based OFDMA is proposed, which forms multiple orthogonal beams with common spatial null in the direction of a victim FSS earth station (ES). The design enables both transmitter and receiver to independently construct identical codebook by sharing only on the direction angle of an FSS ES, which takes fewer overhead bits than Gram-Schmidt process, a general method satisfying our design criterion. A system-level throughput evaluation shows that the proposed precoding provides superior performance over existing spectrum sharing method, that is, subband deactivation. The spectrum sharing analysis shows that the proposed precoding, even with an estimation error of the direction angles of an FSS ES, causes lower interference than existing precoding, knockdown precoding.

Keywords: SDMA-OFDMA, precoder codebook, nullsteering, orthogonal beamforming, limited feedback.

I. Introduction

The International Telecommunication Union for Radiocommunication (ITU-R) has allocated subbands 3.4 GHz to 4.2 GHz, which are allocated to fixed-satellite services (FSS) in many countries around the world, for International Mobile Telecommunications (IMT)-Advanced service [1]. The spectrum sharing results of using a minimum coupling loss (MCL) link budget show that protection distance should be greater than 40 km to avoid mutually harmful interference between two systems operating in the same frequency bands [1]. Since the 40 km is too great from a practical view, an interference mitigation technique is essential. Moreover, ITU requires higher bit rates for IMT-Advanced system: Approximately 100 Mbps and 1 Gbps with high mobility and low mobility for 100 MHz bandwidth, respectively [2]. Therefore, the focus of this work is to propose an IMT-Advanced system archiving the following objects:

Spectrum sharing. Sufficient interference suppression to sustain reliable FSS,

High throughput. Sufficiently high data rate for reliable IMT-Advanced service.

In this paper, an approach based on multiple-input multiple-output (MIMO) and orthogonal frequency-division multiple access (OFDMA) is developed. The two schemes can provide high throughput and facilitate spectrum sharing with FSS by the flexible assignment of radio resource in frequency and space domain.

1. Related Work

Many studies have investigated algorithms to protect existing systems by implementing frequency notching and nullsteering

Manuscript received Feb. 8, 2011; revised Apr. 20, 2011; accepted May 6, 2011.

Han-Shin Jo (phone: +1 512 413 1958, email: han-shin.jo@austin.utexas.edu) is with the Department of Electrical and Computer Engineering, University of Texas at Austin, USA.

http://dx.doi.org/10.4218/etrij.11.0111.0078

beamforming. Frequency notching algorithms include the signal waveform adaptation [3], [4] and the tone deactivation based on OFDM [5], [6]. As these frequency notching algorithms generate notches only in the frequency domain, they cause considerably high throughput loss to mitigate interference when many frequency bands are widely overlapped with existing systems. On the other hand, multiple antenna array using nullsteering can protect existing systems without additional radio resources in frequency or time. Jo and others [7] proposed interference mitigation based on nullsteering for coexistence between IMT-Advanced and FSS. The scheme is effective for interference mitigation, while it decreases the throughput of users located in a direction of interferer or victim system too much because a desired signal as well as interference are suppressed.

Codebook-based precoding is proposed for spatial multiplexing in a single user MIMO channel [8]. In Gaussian MIMO broadcast channels, simultaneous transmission to multiple users, known as multiuser MIMO or space-division multiple access (SDMA), is capable of achieving very high throughput. SDMA is as a candidate for Long Term Evolution (LTE)-Advanced and IMT-Advanced standard [9]. In particular, a codebook-based orthogonal beamforming SDMA has been proposed for the 3GPP-LTE standard [10] and 3GPP2-ultra mobile broadband (UMB) standard called knockdown precoding [11]. In the scheme, based on limited feedback information on the preferred precoding matrix within a codebook and the corresponding signal-to-interference-and-noise ratios (SINRs), the multiuser precoding matrix is selected within a codebook to maximize the sum throughput. The precoding matrix constructs orthogonal beams which improve throughput base on reduction of inter-user interference in homogeneous systems. However, SDMA coexisting with FSS requires suppressing interference between the heterogeneous systems as well as the inter-user interference in homogeneous systems.

2. Contributions

Combining orthogonal beamforming and nullsteering can be an approach for achieving both high data rate and spectrum sharing. We thus propose a systematic design of an SDMA codebook which forms multiple orthogonal beams, that is, orthogonal beamforming constraint, with common null in the direction of a victim FSS earth station (ES), that is, nullsteering constraint. Furthermore, unlike the Gram-Schmidt process, which is a general method for designing SDMA codebook satisfying both constraints, both transmitter and receiver independently construct identical codebook at both ends by sharing the proposed systematic design rule based only on the direction angle of victim FSS ES, which takes fewer overhead bits than the Gram-Schmidt process.

Multiuser precoding and scheduling with limited feedback are extended to subband-based OFDMA. The system employs two SDMA codebooks, that is, one for the subband shared with FSS (interfering subband) and one for the subband not shared (non-interfering subband), which is adaptively selected for each subband. This keeps the feedback overhead and scheduling complexity low and improves the system throughput through the additional utilization of spatial spectrum. Moreover, this improves the throughput of users located in a direction of victim FSS ES, by using the data transmission via non-interfering subband, which is the merit of our scheme over [7].

The remainder of this paper is organized as follows. The system model is described in section II. We design SDMA codebook and user scheduling in section III. In section IV, system-level simulation results are evaluated to show the throughput performance of the proposed SDMA-OFDMA. In section V, we analyze the interference mitigation ability of the SDMA-OFDMA. Finally, conclusions are drawn in section VI.

II. System Model

Since the 3,400 MHz to 4,200 MHz bands are only allocated to downlink (space to earth) FSS, there is no interference from FSS ES to IMT-Advanced systems. Moreover, there is no interesting issue for study regarding interference from geo-stationary orbit (GSO) satellites to IMT-Advanced systems because there is little interference between satellites and earth. We thus consider the interference only from IMT-Advanced base station (BS) to FSS ES.

Figure 1 shows the proposed downlink SDMA-OFDMA system with n_T transmit antennas, n_R receive antennas, M subcarriers, and K users per sector. We assume that the cyclic prefix is larger than the length of channel impulse response such that OFDM modulation decomposes the frequency selective MIMO fading channel into a set of parallel frequency flat fading channels. Encoding and detection for data streams are performed on each subcarrier independently by using feedback on channel quality information (CQI) and radio resource management per subcarrier. To keep the feedback overhead and scheduling complexity low, the total subcarriers are divided into N subbands consisting of M/N consecutive subcarriers. The index for the subband is omitted in the following, as spatial processing is independently performed on a subband basis.

Let $\mathbf{x}$ be $n_T \times 1$ transmitted signal vector. Then, $n_R \times 1$ received signal vector of the k-th user $\mathbf{y}_k$ is given by

$$\mathbf{y}_k = \sqrt{\frac{\rho_k}{n_S}}\mathbf{H}_k\mathbf{x} + \mathbf{n}_k, \quad (1)$$

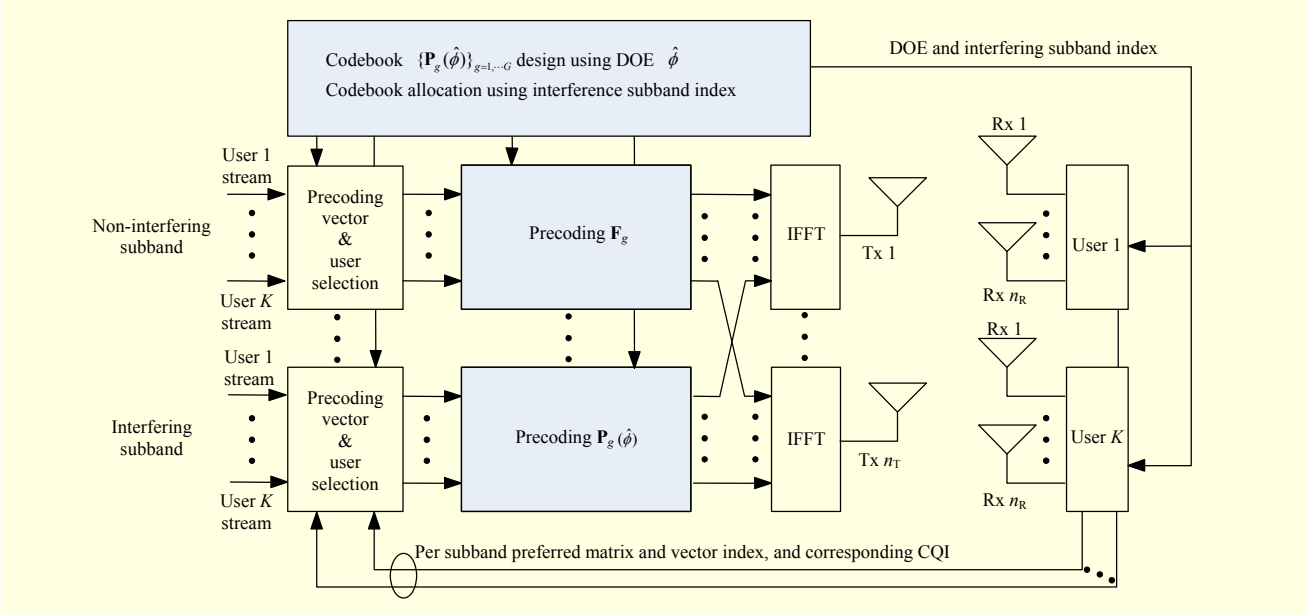

Fig. 1. Proposed codebook-based precoding for SDMA-OFDMA.

where ρ_k is the average received signal to noise ratio (SNR) per receiving antenna, n_S is the number of simultaneous substreams, $\mathbf{H}_k$ is an $n_R \times n_T$ channel matrix, $\mathbf{n}_k$ is an $n_R \times 1$ additive white complex Gaussian noise vector, and the entries of $\mathbf{H}_k$ and $\mathbf{n}_k$ are independent and identically distributed complex Gaussian random variables with zero mean and unit variance. We assume a highly correlated channel from a BS to FWS based on high probability of line-of-sight between them. It facilitates mitigating interference to FSS ES by construction of a transmit null at the BS. For each subband, SDMA transmits n_S substreams to the receivers $\{k_m^*\}_{m=1,\cdots,n_S}$ via the precoding vector $\{\mathbf{w}_m\}_{m=1,\cdots,n_S}$. The transmit signal is then

$$\mathbf{x} = \mathbf{W}\mathbf{s} = \sum_{m=1}^{n_S} \mathbf{w}_m s_m, \qquad (2)$$

where $\mathbf{W} = [\mathbf{w}_1 \cdots \mathbf{w}_{n_S}]$ and $\mathbf{s} = [s_1 \cdots s_{n_S}]^T$. The n_S precoding vectors $\{\mathbf{w}_m\}_{m=1,\cdots,n_S}$ are selected within a precoder codebook, $\mathcal{F}$ or $\mathcal{P}(\hat{\phi})$, using the scheduling algorithm described in section III.4. Subbands are adaptively classified into an interfering subband, that is, the subband currently occupied by FSS), and a non-interfering subband. As shown in Fig. 1, a precoder codebook per subband is selected from $\mathcal{F}=\{\mathbf{F}_1,\cdots,\mathbf{F}_G\}$ (non-interfering subband) and $\mathcal{P}(\hat{\phi})=\{\mathbf{P}_1,\cdots,\mathbf{P}_G\}$ (interfering subband), which designed as described in section III.1. Here, $\hat{\phi}$ is the direction angle of ES (DOE). For the non-interfering subband and the interfering subband, the number of simultaneous substreams n_S is equal to n_T and n_T–1, respectively.

III. SDMA Codebook and User Scheduling

1. SDMA Codebook Design

In this section, a systematic design method is proposed for the construction of the SDMA codebook $\mathcal{P}(\hat{\phi})$ for an interfering subband. Based on the assumptions that the IMT-Advanced BS is already aware of the DOE $\hat{\phi}$ and the interfering subband index, both the BS and users independently construct an identical codebook for an interfering subband at both ends by sharing the codebook design rule, the information of $\hat{\phi}$, and the interfering subband index by downlink broadcasting.

Initially, the BS must obtain the DOE and interfering subband index. The DOE can be obtained by adopting a popular spatial-spectrum estimation direction-finding method [12], [13] or from a database with information concerning the DOE. Moreover, a spectrum sensing technique provides the interfering subband index. In this paper, it is assumed that the DOE and the interfering subband index obtained at the BS are sent to all K users via a downlink control channel. This assumption enables the construction of an identical codebook for the interfering subbands at both ends through sharing of the systematic design method.

To enhance the sum throughput of an SDMA system and to mitigate interference to a victim FSS ES, a precoder codebook for interfering subband, $\mathcal{P}(\hat{\phi}) = \{\mathbf{P}_g(\hat{\phi})\}_{g=1,\cdots,G}$, forms a spatial null at the DOE $\hat{\phi}$, that is, a nullsteering constraint, as well as spatial orthogonal beams, that is, an orthogonal beamforming constraint. Designing the codebook starts from

the SDMA codebook for non-interfering subband $\mathcal{F} = \{\mathbf{F}_1, \cdots, \mathbf{F}_G\}$ (knockdown precoding coodbook [11]). The m-th precoding vector of the g-th matrix $\mathbf{F}_g$ is given by [11]

$$\mathbf{f}_{g,m} = \frac{1}{\sqrt{n_{\mathrm{T}}}} \left[1 \;\; e^{j\frac{2\pi}{n_{\mathrm{T}}}\left(\frac{g-1}{G}+m-1\right)} \cdots e^{j\frac{2\pi}{n_{\mathrm{T}}}\left(n_{\mathrm{T}}-1\right)\left(\frac{g-1}{G}+m-1\right)} \right]^T, \quad (3)$$

where $(\cdot)^T$ represents a transpose operator and G is the number of precoding matrices in the codebook. Note that the precoding matrix $\mathbf{F}_g$ satisfies the orthogonal beamforming constraint only. The transmit gain of $\mathbf{f}_{g,m}$ in the direction ϕ is given by

$$\begin{aligned}\Gamma(\mathbf{f}_{g,m}, \phi) &= |\, \mathbf{f}_{g,m}^T \mathbf{a}(\phi) \,|^2 \\ &= \left| 1/n_{\mathrm{T}} \sum_{k=0}^{n_{\mathrm{T}}-1} e^{j2\pi k\left(\left((g-1)/G+m-1\right)/n_{\mathrm{T}} + d_{\mathrm{T}} \sin\phi/\lambda\right)} \right|^2, \end{aligned} \quad (4)$$

where $\mathbf{a}(\phi)$ is the array steering vector at a angle ϕ. It is given by

$$\mathbf{a}(\phi) = \frac{1}{\sqrt{n_{\mathrm{T}}}} \left[1 \; e^{j2\pi\frac{d_{\mathrm{T}}}{\lambda}\sin\phi} \cdots e^{j2\pi\left(n_{\mathrm{T}}-1\right)\frac{d_{\mathrm{T}}}{\lambda}\sin\phi} \right]^T, \quad (5)$$

where λ is wavelength. The null points ϕ satisfying $\Gamma(\mathbf{f}_{g,m}, \phi) = 0$ have the property described by the following lemma.

Lemma 1. There exist at least one common null point $\phi_g^{(n)}$ such that $\mathbf{f}_{g,m}^T \mathbf{a}(\phi_g^{(n)}) = 0$, for all $m \in \mathcal{M}_n$, where $n_{\mathrm{T}} \geq 2$, $-\pi/2 \leq \phi_g^{(n)} < \pi/2$, and $\mathcal{M}_n = \{1, 2, \cdots, n-1, n+1, \cdots, n_{\mathrm{T}}\}$.

Proof. $\{\mathbf{f}_{g,m}\}_{m=1,\cdots,n_{\mathrm{T}}}$ is a orthonormal basis of an n_{T} dimensional complex vector space $\mathbb{C}^{n_{\mathrm{T}}}$ $(n_{\mathrm{T}} \geq 2)$. It then becomes clear that the vector $\mathbf{f}_{g,n}$ is orthogonal to the $n_{\mathrm{T}}-1$ vectors $\{\mathbf{f}_{g,m}\}_{m\in\mathcal{M}_n}$, that is, $\mathbf{f}_{g,m}^T \mathbf{f}_{g,n} = 0$ for $m \in \mathcal{M}_n$.

At this point, it is shown that at least one $\phi_g^{(n)}$ exists such that $\mathbf{a}(\phi_g^{(n)}) = \mathbf{f}_{g,n}$. The complex exponential function $f(x) = e^{jx}$ has the period of 2π, therefore,

$$\begin{aligned} &2\pi(n_{\mathrm{T}}-1)d_{\mathrm{T}}/\lambda \sin\phi_g^{(n)} \\ &\quad = 2\pi(n_{\mathrm{T}}-1)\left((g-1)/G+m-1\right)/n_{\mathrm{T}} + 2k\pi, \end{aligned}$$

for any integer k to satisfy $\mathbf{a}(\phi_g^{(n)}) = \mathbf{f}_{g,n}$. The equation is rewritten as

$$\sin\phi_g^{(n)} = \lambda\left((g-1)/G+m-1\right)/d_{\mathrm{T}} n_{\mathrm{T}} + k',$$

for any integer k'. Then, without a loss of generality, there is at least one k' such that $|\lambda\left((g-1)/G+m-1\right)/d_{\mathrm{T}} n_{\mathrm{T}} + k'| \leq 1$, which results in the desired results. □

Lemma 1 states that an $n_{\mathrm{T}} \times (n_{\mathrm{T}}-1)$ precoding matrix $\mathbf{Q}_g^{(n)}$ consisting of $n_{\mathrm{T}}-1$ column vectors of $\mathbf{F}_g$, $\{\mathbf{f}_{g,m}\}_{m\in\mathcal{M}_n}$ has an aggregated transmit gain of zero at $\phi_g^{(n)}$ as follows:

$$\Gamma(\mathbf{Q}_g^{(n)}, \phi_g^{(n)}) = \sum_{m\in\mathcal{M}_n} |\, \mathbf{f}_{g,m}^T \mathbf{a}(\phi_g^{(n)}) \,|^2 = 0. \quad (6)$$

Constructing $\{\mathbf{P}_g(\hat{\phi})\}_{g=1,\cdots,G}$ from $\mathbf{Q}_g^{(n)}$ demands adaptive steering of the common null at ϕ_g to the DOE $\hat{\phi}$. Since there is at least one $\phi_g^{(n)}$ for a specific g and n from lemma 1, the reference direction ϕ_g is determined as $\phi_g^{(n)}$ minimizing $|\phi_g^{(n)} - \hat{\phi}|$.

Proposition 1. Nullsteering. The precoding matrix forming a null at the DOE $\hat{\phi}$ for an interfering subband is given by

$$\mathbf{P}_g(\hat{\phi}) = \mathbf{R}_g(\hat{\phi}) \mathbf{Q}_g^{(n)}, \quad (7)$$

where $\mathbf{R}_g(\hat{\phi}) = diag(\mathbf{r}_g(\hat{\phi}))$ is an $n_{\mathrm{T}} \times n_{\mathrm{T}}$ diagonal matrix containing the vector of diagonal entries $\mathbf{r}_g(\hat{\phi})$ given by

$$\begin{aligned} \mathbf{r}_g(\hat{\phi}) = \Bigg[& 1 \;\; e^{-j2\pi\frac{d_{\mathrm{T}}}{\lambda}\cos\hat{\phi}\sin\alpha_g} \left(e^{j2\pi\frac{d_{\mathrm{T}}}{\lambda}\sin\hat{\phi}} \right)^{\cos\alpha_g - 1} \cdots \\ & e^{-j2\pi\left(n_{\mathrm{T}}-1\right)\frac{d_{\mathrm{T}}}{\lambda}\cos\hat{\phi}\sin\alpha_g} \left(e^{j2\pi\left(n_{\mathrm{T}}-1\right)\frac{d_{\mathrm{T}}}{\lambda}\sin\hat{\phi}} \right)^{\cos\alpha_g - 1} \Bigg]^T. \end{aligned} \quad (8)$$

with $\alpha_g = \hat{\phi} - \phi_g$.

Proof. Let $\alpha_g = \hat{\phi} - \phi_g$, the transmit gain of the column vectors of $\mathbf{Q}_g^{(n)}$, $\{\mathbf{f}_{g,m}\}_{m\in\mathcal{M}_n}$ in the direction ϕ_g is then

$$\begin{aligned} \Gamma(\mathbf{f}_{g,m}, \phi_g) &= \Gamma(\mathbf{f}_{g,m}, \hat{\phi} - \alpha_g) \\ &= \left| \frac{1}{n_{\mathrm{T}}} \sum_{k=0}^{n_{\mathrm{T}}-1} e^{j2\pi k\left(\frac{1}{n_{\mathrm{T}}}\left(\frac{g-1}{G}+m-1\right)+\frac{d_{\mathrm{T}}}{\lambda}\sin\left(\hat{\phi}-\alpha_g\right)\right)} \right|^2 \\ &= \Bigg| \frac{1}{n_{\mathrm{T}}} \sum_{k=0}^{n_{\mathrm{T}}-1} \Bigg[e^{j2\pi k\left(\frac{1}{n_{\mathrm{T}}}\left(\frac{g-1}{G}+m-1\right)+\frac{d}{\lambda}\sin\hat{\phi}\right)} \\ &\qquad \times e^{-j2\pi k\frac{d}{\lambda}\cos\hat{\phi}\sin\alpha_g} \left(e^{j2\pi k\frac{d}{\lambda}\sin\hat{\phi}} \right)^{\cos\alpha_g - 1} \Bigg] \Bigg|^2 = 0. \end{aligned} \quad (9)$$

From (4) and (5), (9) is rewritten as

$$\Gamma\left(\mathbf{f}_{g,m}, \phi_g\right) = \left| \left(\mathbf{f}_{g,m} \odot \mathbf{r}_g(\hat{\phi})\right)^T \mathbf{a}(\hat{\phi}) \right|^2 = \Gamma\left(\mathbf{f}_{g,m} \odot \mathbf{r}_g(\hat{\phi}), \hat{\phi}\right), \quad (10)$$

where $\odot$ denotes the Hadamard (pointwise) product. Let the $n_{\mathrm{T}}-1$ column vectors of $\mathbf{P}_g(\hat{\phi})$, $\{\mathbf{p}_{g,k}(\hat{\phi})\}_{k=1,\ldots,n_{\mathrm{T}}-1}$ be $\mathbf{p}_{g,k}(\hat{\phi}) = \mathbf{f}_{g,m} \odot \mathbf{r}_g(\hat{\phi})$, $m \in \mathcal{M}_n$. Thus,

$$\Gamma\left(\mathbf{p}_{g,k}(\hat{\phi}), \hat{\phi}\right) = 0, \quad \text{for all } k \in \{1, \cdots, n_{\mathrm{T}}-1\}. \quad (11)$$

This leads to

$$\Gamma\left(\mathbf{P}_g(\hat{\phi}),\hat{\phi}\right)=\sum_{k=1}^{n_{\mathrm{T}}-1}\Gamma\left(\mathbf{p}_{g,k}(\hat{\phi}),\hat{\phi}\right)=0, \tag{12}$$

which shows that the aggregate transmit gain of $\mathbf{P}_g(\hat{\phi})$ becomes zero at the DOE $\hat{\phi}$. Due to the irrelevance of $\mathbf{r}_g(\hat{\phi})$ to a precoding vector index *m*, the precoding matrix $\mathbf{P}_g(\hat{\phi})$ can be compactly represented as (7). □

The mutual orthonormality of the n_{T} column vectors of $\mathbf{E}_g$ remains for the $n_{\mathrm{T}}-1$ column vectors of $\mathbf{P}_g(\hat{\phi})$, as shown in the following proposition.

Proposition 2. Orthonormality. The $n_{\mathrm{T}}-1$ column vectors of the precoding matrices $\{\mathbf{P}_g(\hat{\phi})\}_{g=1,\cdots,G}$ are mutually orthonormal.

Proof. From (8), each diagonal entry of $\mathbf{R}_g$ has an absolute value of one. Thus, it is shown that

$$\begin{aligned}\mathbf{P}_g^H(\hat{\phi})\mathbf{P}_g(\hat{\phi}) &= \mathbf{Q}_g^{(n)H}\mathbf{R}_g^H(\hat{\phi})\mathbf{R}_g(\hat{\phi})\mathbf{Q}_g^{(n)}\\ &= \mathbf{Q}_g^{(n)H}\mathbf{I}_{n_{\mathrm{T}}}\mathbf{Q}_g^{(n)}\\ &= \mathbf{Q}_g^{(n)H}\mathbf{Q}_g^{(n)}\\ &= \mathbf{I}_{n_{\mathrm{T}}-1},\end{aligned} \tag{13}$$

where $\mathbf{I}_{n_{\mathrm{T}}}$ is an $n_{\mathrm{T}}\times n_{\mathrm{T}}$ identity matrix and $(\cdot)^H$ denotes the conjugate transpose of a matrix. Therefore, the column vectors of $\mathbf{P}_g$ are mutually orthonormal. □

2. Comparison with Gram-Schmidt Process

We consider a conventional design of the precoding matrix $\mathbf{P}_g$ that satisfies nullsteering and orthonormality constraints without resorting to the precoding matrix $\mathbf{F}_g$. The method constructs $n_{\mathrm{T}}-1$ mutually orthonormal vectors that are orthonormal to the array steering vector at the DOE $\hat{\phi}$, $\mathbf{a}(\hat{\phi})$, using the Gram-Schmidt process. Denote $\mathcal{B}=\{\mathbf{B}_1,\cdots,\mathbf{B}_G\}$ as a set of $n_{\mathrm{T}}\times(n_{\mathrm{T}}-1)$ matrices given by $\mathbf{B}_g=[\mathbf{b}_{g,1}\cdots\mathbf{b}_{g,n_{\mathrm{T}}-1}]$. Using the Gram-Schmidt process, we obtain an orthonormal matrix $\mathbf{U}_g=[\mathbf{u}_{g,1},\cdots,\mathbf{u}_{g,n_{\mathrm{T}}-1},\mathbf{a}(\hat{\phi})]$ from $\mathbf{B}_g$ and $\mathbf{a}(\hat{\phi})$. Finally, the desired precoding matrix $\mathbf{P}_g$ is given from $\mathbf{U}_g$, as $\mathbf{P}_g=[\mathbf{u}_{g,1}\cdots\mathbf{u}_{g,n_{\mathrm{T}}-1}]$.

In the method, it is possible to employ a large number of $\{\mathbf{b}_{g,m}\}_{m=1,\cdots,n_{\mathrm{T}}-1}$ for a specific $\mathbf{a}(\hat{\phi})$, resulting in a number of $\mathbf{U}_g$. A way of determining $\{\mathbf{b}_{g,m}\}_{m=1,\cdots,n_{\mathrm{T}}-1}$ is thus essential. When two approaches (random and deterministic vector generation) are considered, random vector generation is not preferable because both the BS and users scarcely ever construct identical $\mathbf{U}_g$ components due to the randomness of $\mathbf{B}_g$ at both ends. On the other hand, deterministic vector generation requires that both the BS and users know $\{\mathbf{b}_{g,m}\}_{m=1,\cdots,n_T-1}$ for all available $\mathbf{a}(\hat{\phi})$ given by a large number of predetermined $\hat{\phi}$ values, which results in a considerable complexity and a large amount of memory space. On the other hand, the proposed design ensures low complexity due to a simple matrix product, as shown in (7). Moreover, both the BS and users independently construct identical codebook at both ends since they share the proposed systematic design rule based on the $\hat{\phi}$ only.

3. Practicality

The proposed design method tends to impose a restriction on the system configuration in terms of the number of transmit antennas. The method requires the number of transmit antennas at the BS to be larger than the number of different DOEs at which FSS ESs are located. However, some countries, such as France, Sweden, Japan, and South Korea, have a limited number (twenty or less) of registered FSS ESs; moreover, these are not contiguous with each other. Therefore, the proposed method is a practical solution for spectrum sharing between IMT-Advanced and FSS in the 3,400 MHz to 4,200 MHz bands.

Some mobile stations near the FSS ES will cause interference to the FSS when considering the IMT-Advanced uplink. As the DOE at a mobile station is not constant due to its mobility, the mobile station must continuously estimate the DOE; this is a heavy burden on the mobile station. Additionally, when each mobile station linked to a BS utilizes a different precoder forming a null in their own DOE, the BS must employ simultaneously different precoders. Therefore, the conventional subband deactivation algorithm in which frequency notches are produced through the deactivation of the interfering subbands is preferable over the proposed method for an uplink interference scenario.

4. Precoding Vector and User Selection with Limited Feedback

Based on the assumption of the channel knowledge of $\mathbf{H}_k$ at the *k*-th user, the precoding matrix $\mathbf{W}_{g_k}$ is determined to maximize multiuser diversity gain at the *k*-th link within a precoder codebook $\mathcal{F}$ or $\mathcal{P}(\hat{\phi})$ as

$$\mathbf{W}_{g_k}=\begin{cases}\arg\max\limits_{\{\mathbf{F}_g\}_{g=1,\cdots,G}}\max\limits_{m=1,\cdots,n_{\mathrm{T}}}\gamma_{k,m}(\mathbf{F}_g)\\ \qquad\text{for non-interfering subband,}\\ \arg\max\limits_{\{\mathbf{P}_g(\hat{\phi})\}_{g=1,\cdots,G}}\max\limits_{m=1,\cdots,n_{\mathrm{T}}-1}\gamma_{k,m}(\mathbf{P}_g(\hat{\phi}))\\ \qquad\text{for interfering subband,}\end{cases} \tag{14}$$

where $\gamma_{k,m}(\mathbf{A})$ denotes the SINR on the *m*-th stream of the

k-th user when using the precoding matrix $\mathbf{A}$. The amount of multiuser diversity gain depends crucially on the upper tail of the SINR distribution of $\gamma_{k,m}$ at each link: the heavier the tail, the more likely a receiver has a strong channel and the larger the multiuser diversity gain [14]. Thus, selecting the precoding matrix that maximizes the maximum SINR among the SINRs of individual streams at each link makes the upper tail of the SINR distribution heavier at each link. The index of the selected precoding matrix g_k is sent back to the BS via feedback bits of $\lceil \log_2 G \rceil$, where $\lceil x \rceil$ is the smallest integer that is larger than or equal to x. Moreover, each user feeds back maximum SINRs $\max_{m=1,\cdots,n_S}\{\gamma_{k,m}(\mathbf{W}_{g_k})\}$ and its stream index m^* to the BS. This is implemented using $\lceil \log_2 n_S \rceil + R$ bits for each feedback instance of the index m^* and the corresponding SINR $\gamma_{k,m^*}(\mathbf{W}_{g_k})$, respectively, where R represents the required bits for the feeding back of a quantized SINR.

At each subband, all K users fall into G groups $\{\mathcal{S}_g\}_{g=1,\cdots,G}$ according to their selected precoding matrix. The users within the same group share the precoding matrix, which makes the feedback information on SINRs from users valid as long as users within the same group are allowed for simultaneous transmission. Within each group $\mathcal{S}_g$, the BS attempts to assign $\{s_m\}_{m=1,\cdots,n_S}$ to n_S users $\{k_m^*\}_{m=1,\cdots,n_S} \in \mathcal{S}_g$ with the highest SINR per beam. The instantaneous sum throughput of the group $\mathcal{S}_g$ using the precoding matrix $\mathbf{W}_g$ is given by

$$T(\mathbf{W}_g) = \sum_{m=1}^{n_S} \log_2\left(1+\gamma_{k_m^*,m}(\mathbf{W}_g)\right). \quad (15)$$

Finally, the unitary precoding matrix $\mathbf{W}$ used for transmission is determined at each subband to maximize the instantaneous system throughput by

$$\mathbf{W} = \arg \max_{\{\mathbf{W}_g\}_{g=1,\cdots,G}} T(\mathbf{W}_g). \quad (16)$$

The final instantaneous system throughput is given by summing up $T(\mathbf{W})$ over all subbands.

IV. System Throughput Evaluation

By evaluating the average sum throughput through system level simulation, the superiority of the proposed interference mitigation algorithm over the conventional subband deactivation algorithm is demonstrated.

1. Channel Model

The spatial channel model (SCM) was developed to define spatial channel characteristics and a system level simulation methodology for a single-carrier MIMO system by an ad-hoc group comprised of participants of the 3GPP and 3GPP2 [15]. For evaluating multicarrier MIMO systems, the SCM proposed for a single-carrier MIMO system is extended here to that for a multicarrier MIMO system. For a sector-mobile pair, L multipath channel matrices $\{\mathbf{H}_{k,l}\}_{l=1,\cdots,L}$ with delays $\{\tau_l\}_{l=1,\cdots,L}$ are generated by the SCM and quantized to T_s/M in time, where T_s and M denote the interval of an OFDM symbol and the number of subcarriers, respectively. The quantized M samples $\{\hat{\mathbf{H}}_{k,m}\}_{m=1,\cdots,M}$ are transformed into the channel matrices of M subcarriers $\{\tilde{\mathbf{H}}_{k,m}\}_{m=1,\cdots,M}$ by the discrete Fourier transform (DFT). The spatial correlation characteristics of a single-carrier MIMO channel are preserved over the DFT process. In this work, spatial parameters according to the given random distributions defined by the SCM are used.

2. Simulation Methodology

An OFDMA cellular network based on IEEE 802.16e assumptions with two rings of three-sector BSs is considered for high-speed downlink packet data services. Table 1 summarizes the default simulation parameters.

The four-elements linear antenna array is assumed at both the transmitter and receiver with antenna spacing of 0.5λ, respectively. At each drop, users are randomly distributed throughout the system and are connected to the BS with the smallest integral path loss among all possible links to the BSs. For the duration of a drop, the simulation operates at the frame level. At each frame, MIMO-OFDM channel coefficients of all possible links, including both desired and interference links, are generated by the multicarrier SCM. The proposed interference mitigation algorithm and SDMA operation is performed on the basis of a subband, which consists of 64 data subcarriers and 8 pilot subcarriers. Modulation used in the simulations are QPSK, 16 QAM, and 64 QAM, all turbo encoded. Transmission rates are decided based on the SNR that is required by each MCS to achieve the 1% of desired target FER in the AWGN channel. The average sum throughput is obtained by averaging the average transmission rates, each of which is computed by averaging the instantaneous transmission rates over 6,000 frames (30 s) for a drop, over 300 independent drops.

3. Simulation Results

The average sum throughput of the downlink OFDMA system with 4×4 SDMA using the precoding matrix $\mathbf{F}_1$ and $\mathbf{P}_1$ ($\hat{\phi} = 30^\circ$) is evaluated in an urban 8º macro environment. We assume that a single FSS ES is at the cell edge and

Table 1. System parameters for simulation.

Parameters	Values
Cell structure	57 hexagonal grid sectors (2-ring, 3-sector, 19 cells)
Site-to-site distance	1 km
BS antenna pattern	70 ° (–3 dB) with 20 dB front-to-back ratio
BS antenna gain (with cable loss)	15 dBi
User antenna gain	–1 dBi
User noise figure	7 dB
Thermal noise density	–174 dBm/Hz
Center frequency	2.3 GHz
Channel model	Multicarrier SCM
Bandwidth	10 MHz
Number of Tx. antennas	4
Number of Rx. antennas	4
Total BS power	20 W
Traffic ch. power ratio	84%
Number of total subcarriers	1,024 (data: 768, pilot: 96, guard: 160)
User velocity	3 km/h
Number of subbands for a frame	12
Number of OFDM symbols for a frame	18
Traffic model	Full buffer ftp
MCS feedback delay	15 ms (= 3 frames)

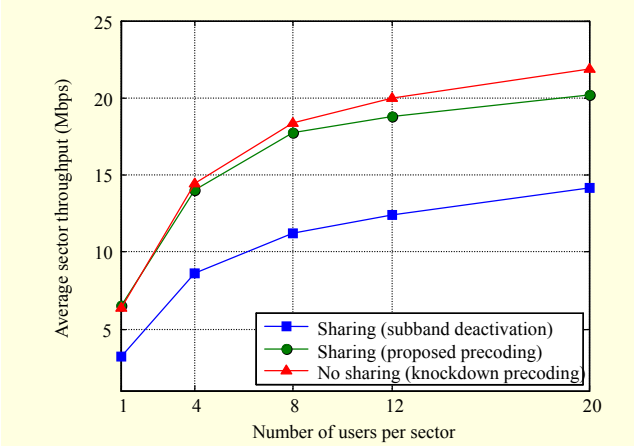

Fig. 2. Average sector throughput versus number of users per sector.

occupies the frequency bands corresponding to 4 subbands out of total 12 subbands. Therefore, the proposed precoding uses $\mathbf{P}_1$ ($\hat{\phi} = 30^\circ$) for data transmission via the 4 subbands, but the

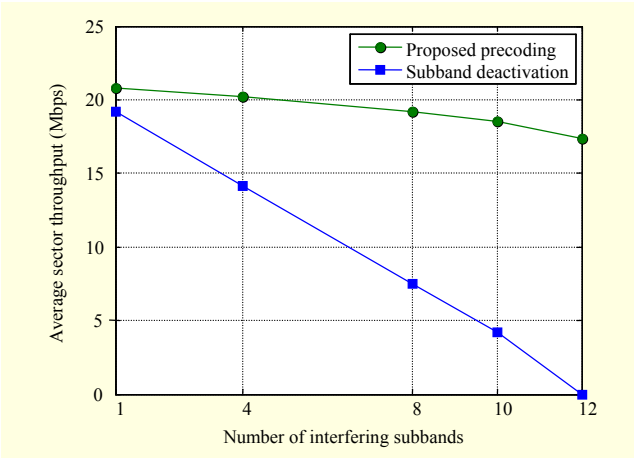

Fig. 3. Average sector throughput versus number of interfering subbands.

subband deactivation does not use the 4 subbands. The knockdown precoding uses $\mathbf{F}_1$ for all subbands.

Figure 2 compares the average sum throughput of the proposed precoding to subband deactivation. The performance of no sharing (knockdown precoding) is also depicted for a reference.

The BS with knockdown precoding simultaneously supports at most four users for each subband by adopting four precoding vectors. On the other hand, the proposed precoding serves at most three users per subband in interfering subbands, and at most four users per subband in non-interfering subbands. Additionally, the BS with the subband deactivation transmits data via non-interfering subbands only. Therefore, both the throughput of the proposed precoding and subband deactivation are lower than that of no sharing, as shown in Fig. 2. Moreover, the proposed precoding achieves throughput gain of up to the 150% compared to the subband deactivation algorithm because the precoding enables the BS to transmit data for interfering subbands.

The average sum throughput of the proposed precoding and the subband deactivation for the number of interfering subbands are shown in Fig. 3. The number of users per sector is assumed to be 20. Although the throughput of both schemes decreases as the number of interfering subbands increases, throughput enhancement of the precoding over subband deactivation is more remarkable at a larger number of interfering subbands. In particular, for 12 interfering subbands, the throughput of subband deactivation is zero, while the proposed precoding provides considerable performance. These results indicate that the proposed precoding is robust against increase in the number of interfering subbands and provides consistently superior performance compared to conventional subband deactivation.

The simulation results show the throughput for a low-

mobility user (3 km/h). All the schemes considered would provide less throughputs at higher speed, since faster channel variation reduce the accuracy of CQI and precoding matrix reported from the users.

V. Spectrum Sharing Analysis

1. Protection Distance

An assessment of spectrum sharing is based on the concept of permissible interference power at the antenna terminals of a victim system. Hence, the attenuation required to limit the level of interference from an interfering system to the permissible interference power for p% of the time is represented by the minimum required loss. This is the loss that needs to be equaled or exceeded by the predicted path loss for all but p% of the time [16]. When p is a small percentage of the time in a range of 0.001% to 1.0%, the interference is referred to as short term; it is referred to as long term for $p \geq 20\%$.

The minimum required loss $L_{\min}$ in dB is described by

$$L_{\min} = P_{BS} + G_{BS} + G_{FS} + L_r - I_{\max}, \quad (17)$$

where P_{BS} is the transmit power of IMT-Advanced BSs (dBW) in the reference bandwidth, $I_{\max}$ is the maximum permissible interference power (dBW) in the reference bandwidth to be exceeded for no more than the percentages of the time at the terminals of the antennas of the receiving FSS ESs, and G_{FS} is the FSS ES antenna gain in the IMT-Advanced BS direction. The IMT-Advanced BS antenna gain in the FSS ES direction is G_{BS} and can be expressed as

$$G_{BS} = G_{ANT}(\phi) + G_{BF}(\phi). \quad (18)$$

The conventional BS antenna pattern without the interference mitigation technique, $G_{ANT}(\phi)$ $(-180^\circ \leq \phi \leq 180^\circ)$ is specified by [17]

$$G_{ANT}(\phi) = G_{\max} - \min[12(\phi/\phi_{3dB})^2, A_m], \quad (19)$$

where the maximum antenna gain $G_{\max}$ is 42.5 dBi, the 3 dB bandwidth ϕ_{3dB} is 70°, and the maximum attenuation A_m is 20 dB. $G_{BF}(\phi)$ has adaptive beamforming patterns generated by the proposed interference mitigation technique. It can be expressed as

$$G_{BF}(\phi) = 20\log_{10}\left|\frac{P_{BS}}{n_T - 1}\sum_{k=1}^{n_T-1}\mathbf{p}_{g,k}^T\mathbf{a}(\phi)\right|. \quad (20)$$

The interfering signal power loss is L_r, which accounts for the fraction of interfering signal power that appears in the band of the victim system in a dB scale. The interfering signal power loss for the interfering system with OFDM is derived through a power spectral density (PSD) analysis of the OFDM signals [18, (10)]. This formula is derived in series form and is implemented simply with the help of simulation, resulting in significantly reduced time to obtain the solution.

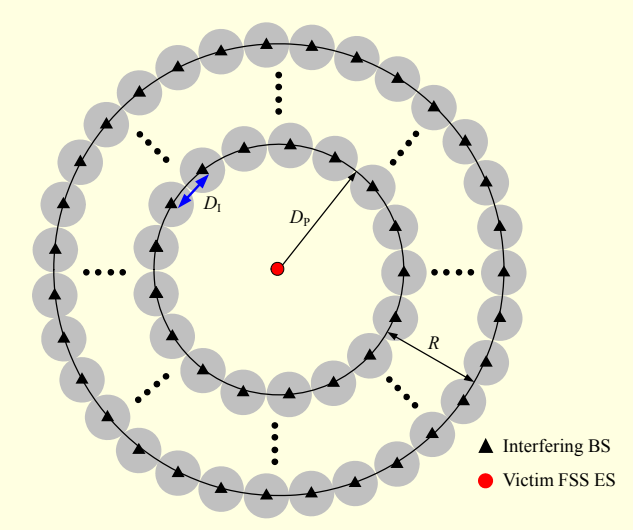

Fig. 4. Interference scenario: multiple IMT-Advanced BS.

The result of the interference calculation is the minimum required loss. Having chosen an appropriate path loss model, this can subsequently be converted into a minimum physical separation distance between interfering and victim systems that is, protection distance. The standard model agreed upon in the ITU and CEPT for terrestrial interference assessment at microwave frequencies is clearly denoted in the ITU-R recommendation P.452-12 [19]. Therefore, the P.452 model is used for the frequency sharing study.

2. Simulation Setup

We consider typical FSS parameters defined in the ITU-R [20]. The system occupies a bandwidth of 5 MHz assigned with a center frequency of 3.5 GHz. A dish-shaped directional antenna with a diameter of 3.8 m and a maximum antenna gain of 41 dBi is deployed. Antenna patterns are modeled mathematically for use in an interference assessment in cases where the ratio between the antenna diameter and the wavelength is less than or equal to 100 $(D/\lambda \leq 100)$ in [21]. The permissible long-term interference power is considered to be −153.8 dBW/5 MHz and is calculated based on I/N= −12.2 dB [22]. A 3-sector IMT-Advanced BS with a bandwidth of 10 MHz in rural environments is assumed. Moreover, IMT-Advanced BS with 4 transmit antennas is able to support the interference mitigation of the proposed SDMA-OFDMA. The transmit power is 13 dBW, and the maximum antenna gain, including a 4 dB feeder loss, is 12 dBi. The

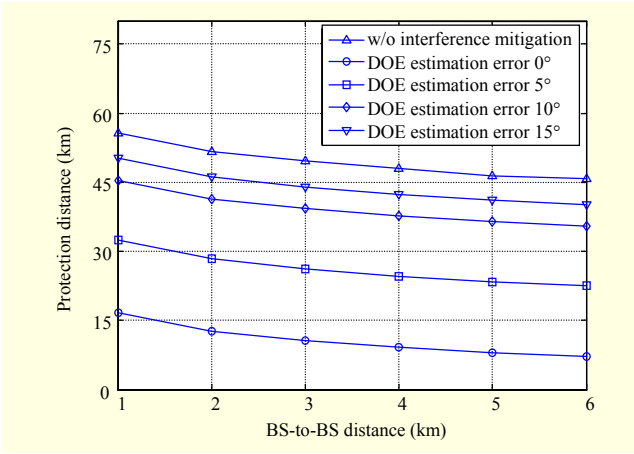

Fig. 5. Protection distance of proposed precoding with interference mitigation, knockdown precoding represents the case of without interference mitigation.

antenna height is 15 m.

Here, we consider the cochannel and adjacent channel interference scenario. Figure 4 describes an aggregated interference scenario caused by multiple IMT-Advanced BSs. The BSs are uniformly (equi-spaced) located on rings around the FSS ES. The aggregated interference takes into account the interference from all BSs located up to the farthest ring. The distance between the closest and the farthest ring R is assumed to be 20 km. The radius of the closest ring is the required protection distance D_p resulting from the calculation of the total sum of the interference contribution.

3. Simulation Results

Figure 5 shows the protection distance D_p as a function of BS intersite distance D_I for the cochannel scenario.

The number of interfering IMT-advanced BSs decreased as D_I increases, which results in a decrease in D_p. The proposed algorithm with perfect DOE estimation remarkably reduces D_p to 7.2 km to 16.6 km, as compared with 45.8 km to 55.7 km for the case without the interference mitigation, that is, knockdown precoding. Note that the subband deactivation can provide very low protection distance of about zero.

The impact of the DOE estimation error on the performance of interference mitigation is also analyzed in Fig. 5. We clearly observe that an increase in the DOE estimation error produces a greater protection distance. Up to a DOE estimation error of 15º, the protection distance with the interference mitigation is shorter than that without the interference mitigation. We also observe that at a DOE estimation error of 5º, the protection distance can be reduced to about 49% to 58% compared to the case without the interference mitigation. These results indicate that, although highly decreased protection distances are obtained with help of the proposed interference mitigation, complete frequency sharing between two systems is not provided. Though not providing a complete spectrum sharing, the proposed interference mitigation reduces the protection distance by about 50% without any additional radio spectrum resources necessary.

Table 2. Protection distance for the adjacent channel: (a) 1 km BS intersite distance and (b) 6 km BS intersite distance.

Interference mitigation (with: ○, without: ×)	DOE estimation error (°)	Protection distance (km)		
		0 MHz GB	5 MHz GB	10 MHz GB
○	0	1.1	0.089	0.049
○	5	13.2	5.6	3.9
○	10	25.9	17.7	15.5
×	N/A	36.2	27.9	25.7

(a)

Interference mitigation (with: ○, without: ×)	DOE estimation error (°)	Protection distance (km)		
		0 MHz GB	5 MHz GB	10 MHz GB
○	0	0.062	0.021	0.019
○	5	4.3	0.57	0.29
○	10	16.1	8.2	6.3
×	N/A	26.3	18	15.9

(b)

We consider the guard band (GB) variation from 0 MHz to 10 MHz in adjacent channel interference scenario. In Table 2, for all GBs, the protection distances are less than 1.1 km for the perfect DOE estimation. On the other hand, the protection distance for a 10 MHz GB is 15.9 km to 25.7 km without the interference mitigation, that is, spectrum sharing is possible for a GB of much more than 10 MHz. In conclusion, the proposed interference mitigation saves the spectrum resources more than 10 MHz.

VI. Conclusion

We proposed codebook-based precoding for SDMA-OFDMA to mitigate interference to an FSS ES as well as to support a high data rate. The codebook forms multiple orthogonal beams with a common null in the direction of a victim FSS ES. The proposed precoding provides 150% higher system throughput than frequency subband deactivation. Moreover, the precoding is robust against an increase in the number of interfering subbands when compared to the subband deactivation. The proposed precoding reduces the protection

distance by at least 70% (no DOE estimation error) or 50% (DOE estimation error) of knockdown. Both knockdown precoding for all subbands and subband deactivation have weaknesses: higher protection distance due to strong interference of knockdown precoding and lower downlink throughput due to partial usage of subbands. The proposed precoding reaches a compromise between system throughput and spectrum sharing. The proposed precoding requires additional side information of DOE and interfering subband index in comparison with the knockdown precoding. However, since the information is static, it is sent to users only once. Thus, the weakness of the additional information is minor.

References

[1] ITU-R Report M.2109, "Sharing Studies Between IMT Advanced Systems and Geostationary Satellite Networks in the Fixed-Satellite Service in the 3 400-4 200 and 4 500-4 800 MHz Frequency Bands," Aug. 2007.

[2] ITU-R WP 8F/TEMP/290, "Preliminary Draft New Report on Radio Aspects for the Terrestrial Component of IMT-2000 and Systems beyond IMT-2000," Oct. 2005.

[3] V.D. Chakravarthy et al., "Multiple Signal Waveforms Adaptation in Cognitive Ultra-Wideband Radio Evolution," *Proc. IEEE WCNC*, Apr. 2005, pp. 724-729.

[4] H. Zhang et al., "Multiple Signal Waveforms Adaptation in Cognitive Ultra-Wideband Radio Evolution," *IEEE J. Sel. Areas Commun*., vol. 24, no. 4, Apr. 2006, pp. 878-884.

[5] T.A. Weiss and F.K. Jondral, "Spectrum Pooling: An Innovative Strategy for the Enhancement of Spectrum Efficiency," *IEEE Commun. Mag*., vol. 42, no. 3, Mar. 2004, pp. S8-S14.

[6] A. Batra, S. Lingam, and J. Balakrishnan, "Multi-band OFDM: A Cognitive Radio for UWB," *Proc. IEEE ISCAS*, May. 2006, pp. 4094-4097.

[7] H.-S. Jo et al., "Coexistence Method to Mitigate Interference from IMT-Advanced to Fixed Satellite Service," *Wireless Technologies, European Conf.*, 2007, pp. 158-161.

[8] D.J. Love and R.W. Heath, "Limited Feedback Unitary Precoding for Spatial Multiplexing Systems," *IEEE Trans. Info. Theory*, vol. 51, no. 8, Aug. 2005, pp. 2967-2976.

[9] 3GPP, *FDD RIT Component of SRIT LTE Release 10 & beyond (LTE-Advanced), RP-090739*, Sept. 2009. Available: http://www.3gpp.org/ftp/tsg ran/TSG RAN/TSGR 45/ Documents/RP-090739.zip

[10] Samsung Electronics, "Downlink MIMO for EUTRA," in 3GPP TSG RAN WG1 R1-060335, Feb. 2006.

[11] 3GPP2, "Physical Layer for Ultra Mobile Broadband (UMB) Air Interface Specification," in 3GPP2 C.S0084-001-0, Apr. 2007.

[12] J.A. Fessler and A.O. Hero, "Space-Alternating Generalized Expectation-Maximization Algorithm," *IEEE Trans. Signal Process.*, vol. 42, no. 10, Oct. 1994, pp. 2664-2677.

[13] P. Chevalier, A. Ferreol, and L. Albera, "High-Resolution Direction Finding from Higher Order Statistics: The 2q-MUSIC Algorithm," *IEEE Trans. Signal Process.*, vol. 54, no. 8, Aug. 2006, pp. 2986-2997.

[14] P. Viswanath, D.N.C. Tse, and R. Laroia, "Opportunistic Beamforming Using Dumb Antennas," *IEEE Trans. Inf. Theory*, vol. 48, no. 6, June 2002, pp. 1277-1294.

[15] 3GPP-3GPP2 Spatial Channel Model Ad-Hoc Group, *Spatial Channel Model Text*, in SCM-134, April 22, 2003.

[16] ITU-R Rec. SF.1006, "Determination of the Interference Potential between Earth Stations of the Fixed-Satellite Service and Stations in the Fixed Service," Apr. 2003.

[17] 3GPP2/TSG-C.R1002, "1xEV-DV Evaluation Methodology (V12.1)," NOKIA, 2003.

[18] H.-S. Jo et al., "The Coexistence of OFDM-Based Systems beyond 3G with Fixed Service Microwave Systems," *J. Commun. Netw.*, vol. 8, no. 2, June 2006, pp. 187-193.

[19] ITU-R Rec. P.452-12, "Prediction Procedure for the Evaluation of Microwave Interference between Stations on the Surface of the Earth at Frequencies above about 0.7 GHz," Mar. 2005.

[20] ITU-R Rec. S.1328-4, "Satellite System Characteristics to be Considered in Frequency Sharing Analyses within the Fixed-Satellite Service," Sept. 2002.

[21] ITU-R Rec. SM.1448, "Determination of the Coordination Area around an Earth Station in the Frequency Bands between 100 MHz and 105 GHz," May 2000.

[22] ITU-R Rec. S.1432, "Apportionment of the Allowable Error Performance Degradations to Fixed-Satellite Service (FSS) Hypothetical Reference Digital Paths Arising from Time Invariant Interference for Systems Operating below 15 GHz," Jan. 2000.

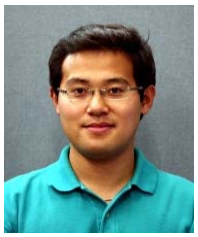

Han-Shin Jo received the BS, MS, and PhD in electrical and electronics engineering from Yonsei University, Seoul, Rep. of Korea, in 2001, 2004, and 2009, respectively. He is currently a postdoctoral fellow in the Department of Electrical and Computer Engineering, University of Texas, Austin. His expertise is in theoretical and practical aspects of multiuser wireless systems and networks. His research interests include theoretical analysis and interference management for femtocell/heterogeneous cellular networks, theoretical analysis and transmission and resource allocation algorithms for MIMO/network and MIMO systems, and stochastic geometry models for radio interference in wireless networks.